

*Research Articles: Behavioral/Cognitive*

## Oscillation-Based Connectivity Architecture Is Dominated by an Intrinsic Spatial Organization, Not Cognitive State or Frequency

<https://doi.org/10.1523/JNEUROSCI.2155-20.2020>

**Cite as:** J. Neurosci 2020; 10.1523/JNEUROSCI.2155-20.2020

Received: 15 August 2020

Revised: 10 October 2020

Accepted: 3 November 2020

---

*This Early Release article has been peer-reviewed and accepted, but has not been through the composition and copyediting processes. The final version may differ slightly in style or formatting and will contain links to any extended data.*

**Alerts:** Sign up at [www.jneurosci.org/alerts](http://www.jneurosci.org/alerts) to receive customized email alerts when the fully formatted version of this article is published.



## Abstract

Functional connectivity of neural oscillations (oscillation-based FC) is thought to afford dynamic information exchange across task-relevant neural ensembles. Although oscillation-based FC is classically defined relative to a pre-stimulus baseline, giving rise to rapid, context-dependent changes in individual connections, studies of distributed spatial patterns show that oscillation-based FC is omnipresent, occurring even in the absence of explicit cognitive demands. Thus, the issue of whether oscillation-based FC is primarily shaped by cognitive state or is intrinsic in nature remains open.

Accordingly, we sought to reconcile these observations by interrogating the ECoG recordings of 18 pre-surgical human patients (8 females) for state-dependence of oscillation-based FC in five canonical frequency bands across an array of six task states.

FC analysis of phase and amplitude coupling revealed a highly similar, largely state-invariant (i.e. intrinsic) spatial component across cognitive states. This spatial organization was shared across all frequency bands. Crucially however, each band also exhibited temporally independent FC dynamics capable of supporting frequency-specific information exchange.

In conclusion, the spatial organization of oscillation-based FC is largely stable over cognitive states, i.e. primarily intrinsic in nature, and shared across frequency bands. Taken together, our findings converge with previous observations of spatially invariant patterns of FC derived from extremely slow and aperiodic fluctuations in fMRI signals. Our observations indicate that “background” FC should be accounted for in conceptual frameworks of oscillation-based FC targeting task-related changes.

## Significance statement

A fundamental property of neural activity is that it is periodic, enabling functional connectivity (FC) between distant regions through coupling of their oscillations. According to task-based studies, such oscillation-based FC is rapid and malleable to meet cognitive task demands. Studying distributed FC

42 patterns instead of FC in few individual connections, we found that oscillation-based FC is largely stable  
43 across various cognitive states and shares a common layout across oscillation frequencies. This stable  
44 spatial organization of FC in fast oscillatory brain signals parallels the known stability of fMRI-based  
45 intrinsic FC architecture. Despite the observed spatial state- and frequency-invariance, FC of individual  
46 connections was temporally independent between frequency bands, suggesting a putative mechanism for  
47 malleable frequency-specific FC to support cognitive tasks.

## 48 49 **Introduction**

50 Oscillation-based functional connectivity (FC) is thought to be essential for neuro-cognitive processing  
51 (Engel et al. 2013; Singer 1999; Varela et al. 2001). Depending on the particular frequency band, such  
52 FC supports performance in the broadest range of cognitive and behavioral domains, from perception  
53 and motor output (Khanna and Carmena 2015; VanRullen 2016) to attention (Jensen et al. 2014; S. Palva  
54 and Palva 2007; Sadaghiani and Kleinschmidt 2016) and language processing (Rimmele et al. 2018).  
55 Oscillation-based FC leverages a fundamental property of electrophysiological activity, namely its  
56 periodicity in characteristic frequency bands. This reliance on neural oscillations dissociates oscillation-  
57 based FC from FC measures derived from broad-band and aperiodic signals (e.g. Pearson correlation)  
58 extensively used in functional magnetic resonance imaging (fMRI) (M. D. Fox and Raichle 2007) as  
59 well as some neurophysiological studies (e.g. Chu et al. 2012). Oscillation-based FC can be  
60 conceptualized in terms of two major modes (Engel et al. 2013; Mostame and Sadaghiani 2020): (1)  
61 phase coupling denoting synchronization of the phase of neural activity of distinct brain regions over  
62 multiple consecutive oscillation cycles (Lachaux et al. 1999; Nolte et al. 2004), and (2) amplitude  
63 coupling denoting synchronization of the magnitude of neural oscillations between regions (Brookes et  
64 al. 2011).

65 Oscillation-based phase- and amplitude coupling have traditionally been evaluated in a connection-wise  
66 manner across a small set of brain regions (Singer, 1999; Uhlhaas et al., 2009). A more recent advance is

67 to derive large-scale connectivity maps from electroencephalography (EEG) or magnetoencephalography  
68 (MEG) source space (e.g. Deligianni et al. 2014; Hipp and Siegel 2015; P. Tewarie et al. 2016) and  
69 intracranial data (Betz et al. 2019; Kucyi et al. 2018). This advance is grounded in the understanding  
70 that the comprehensive FC organization is of functional importance, in part reflecting prior knowledge  
71 stored in the connectome (Sadaghiani and Kleinschmidt 2013; Singer 2013).

72 Such investigations of distributed patterns of oscillations-based FC are commonly applied to the task-  
73 free resting state. At rest, brain oscillations persist to an overall similar extent than during explicit tasks  
74 (although their specific spectral distribution is modulated by cognitive demands). In the following, we  
75 collectively refer to task-free wakefulness and engagement in different behavioral tasks as cognitive  
76 states. For a century, task-independent ongoing oscillations have been the hallmark of EEG (Berger  
77 1930). The spectral profile of this ongoing activity and its cross-areal connectivity have proven  
78 informative for understanding brain function and dysfunction (Kanda et al. 2009; Sadaghiani et al.  
79 2019). Source-localized MEG and EEG studies have reported the presence of a distributed spatial  
80 organization or “architecture” of oscillation-based FC at resting state (Colclough et al. 2016; Hillebrand  
81 et al. 2012; Sockeel et al. 2016; Wirsich et al. 2017). Intracranial cortical surface recordings of  
82 presurgical patients (electrocorticography or ECoG) have confirmed this architecture (Betz et al. 2019;  
83 K. C. Fox et al. 2018; Kucyi et al. 2018) in the absence of the ill-posed problem of EEG/MEG source-  
84 reconstruction (J. M. Palva et al. 2018; Schoffelen and Gross 2009). However, these studies have not  
85 quantitatively assessed (dis)similarity of oscillation-based FC organization across different cognitive  
86 states; Instead, contrasts across task conditions or between post-stimulus and pre-stimulus intervals are  
87 typically investigated in a connection-wise manner. Therefore, the degree to which large-scale FC  
88 organization of oscillatory rhythms is modulated by cognitive context is largely unknown.

89 To summarize, electrophysiological oscillations and their FC express strong context-dependent  
90 flexibility on the one hand and are omnipresent across all cognitive states on the other. This tension

91 therefore begs the question of whether oscillation-based FC is largely governed by a state-invariant, i.e.  
92 intrinsic, spatial organization or is primarily dependent on cognitive demands.

93 A few neurophysiological studies have taken important steps towards answering this question. Kramer et  
94 al. analyzed daylong ECoG recordings across various levels of arousal and states of consciousness  
95 (2011). Static FC across electrodes during periods >100 secs displayed consistent spatial organization  
96 over the course of the day. However, this study did not directly and quantitatively contrast FC across the  
97 different consciousness levels. A subsequent scalp EEG study identified high spatial correlation of static  
98 (>100s) FC organization in sensor space over different sleep stages and wakefulness ( $r>0.75$ ) (Chu et al.  
99 2012). However, different cognitive activities were not dissociated during the waking period. It is  
100 therefore unclear how these findings relate to trial-based oscillatory FC commonly investigated in  
101 cognitive neuroscience. A more recent scalp EEG study showed that phase coupling in reconstructed  
102 source-space is consistent across tasks (resting state, video viewing, and flashing gratings), with FC  
103 clusters that are reproducible across frequency bands (Nentwich et al. 2020). However, while promising  
104 the latter two studies must be interpreted with care due to the methodological limitations imposed by  
105 EEG recorded over the scalp, which may lead to spurious FC even in source space (J. M. Palva et al.  
106 2018). Taken together, these findings motivate direct comparison of static FC organization across  
107 cognitive states using high fidelity intracranial data.

108 Dependence on cognitive context has been well quantified in another research field, namely the study of  
109 very slow FC derived from aperiodic Blood Oxygen Level Dependent (BOLD) fluctuations observed  
110 with fMRI. The brain at resting state displays co-variation in BOLD signals across specific sets of  
111 regions, i.e. intrinsic connectivity networks (Beckmann et al. 2005). Importantly, this intrinsic functional  
112 architecture is also present during task, suggesting that task-specific changes to the brain's fMRI-derived  
113 FC spatial organization are small (Cole et al. 2014; Gratton et al. 2018; Hearne et al. 2017; Smith et al.  
114 2009). For example, Cole et al. (2014) identified a strong spatial correlation ( $r\sim 0.9$ ) between the static  
115 FC organization of rest and task data.

116 However, whether these fMRI-based findings can inform about potential state-invariance in oscillation-  
117 based FC is questionable, given that fMRI-derived FC is an indirect measure of neural activity based on  
118 aperiodic fluctuations of the BOLD signal in the infra-slow range (mainly  $<0.01\text{Hz}$ ) (M. D. Fox and  
119 Raichle 2007; Thompson and Fransson 2015). In contrast, FC as measured by electrophysiological  
120 methods reflects real-time neural processes driven by cyclic activity. As such, oscillation-based FC is  
121 well-positioned to support long-range communication required for cognitive processes that unfold on the  
122 rapid timescale of tens to hundreds of milliseconds (Fell and Axmacher 2011; Gruber et al. 2018;  
123 Uhlhaas et al. 2009). Given these fundamentally different characteristics of the processes associated with  
124 fMRI-based and oscillation-based FC, the degree of context-dependence of the latter requires dedicated  
125 investigation.

126 Another characteristic of fundamental functional importance unique to oscillation-based FC is its  
127 frequency-dependence. In particular, within the context of different tasks specific, cognitive functions  
128 are associated with oscillatory processes in distinct frequencies (e.g. Palva and Palva 2007; Rohenkohl,  
129 Bosman, and Fries 2018). Based on this functional specificity of particular oscillation bands and their  
130 association with different brain regions, should we expect the oscillation-based FC organization in  
131 different frequency bands to differ from each other? This question remains largely unanswered because  
132 task-based studies traditionally focus on task-related modulations in individual connections, ignoring the  
133 distributed spatial organization of oscillation-based FC. The observation of a spatial organization shared  
134 across frequency bands has implications for the neurobiological understanding of functional networks.  
135 Specifically, such frequency-invariance, if observed, would suggest that large-scale functional networks  
136 may enact connectivity in all canonical frequencies irrespective of the sensory, motor, or cognitive  
137 operation that they subserve and the regions that they connect.

138 In light of the foregoing, we addressed two central questions in the current study: (1) is the spatial  
139 organization of fast oscillation-based FC primarily driven by cognitive operations or is it stable across  
140 task states?; (2) is this organization dependent on oscillation frequency? Following these two central

141 investigations, we further asked (3) does frequency-invariant FC organization (if observed) reflect a  
142 single broadband coupling process or truly multiple temporally independent and frequency-specific  
143 processes within a universal spatial organization?; and finally, (4) does the hypothesized stability of  
144 static FC organization over cognitive states and frequency bands depend on the specific connectivity  
145 mode, i.e., phase- or amplitude coupling? To address these questions while minimizing the impact of  
146 volume conduction on FC (J. M. Palva et al. 2018; Schoffelen and Gross 2009), we study ECoG in  
147 patients undergoing clinical evaluation for epilepsy surgery. We further replicate major findings using  
148 additional FC measures that suppress the impact of potential volume conduction. In summary, we  
149 dissociate among four possible scenarios of state- and frequency-dependency of FC organization as  
150 illustrated in Fig.1.



## Materials and Methods

157

### Data

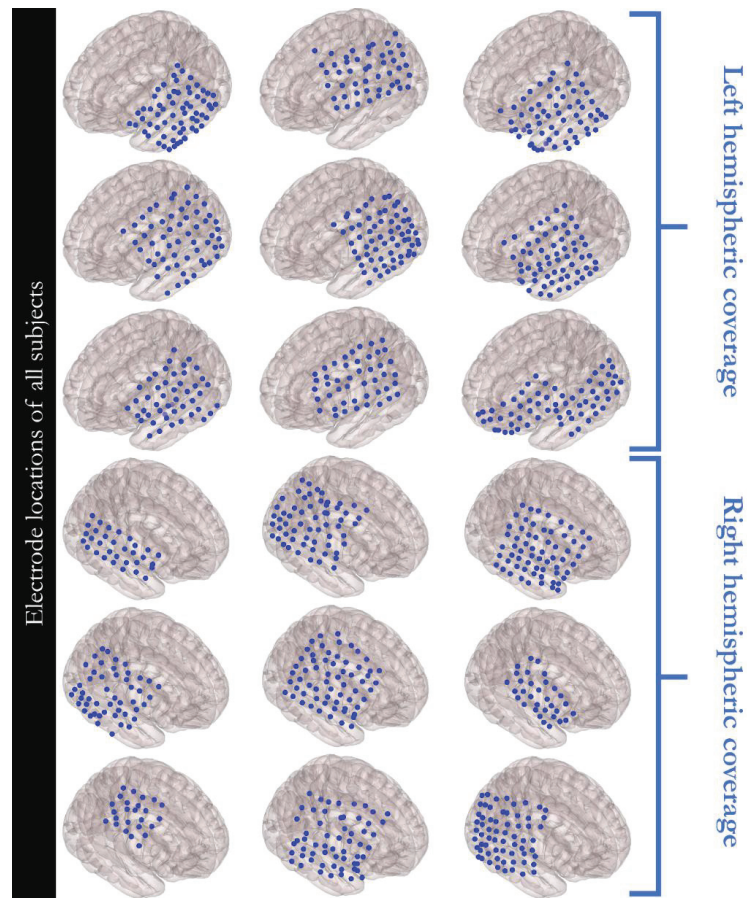
158

159 In this study, we used publicly available ECoG recordings during resting state and 3 independent  
160 paradigms comprising a total of 6 distinct cognitive states. The data is described in detail in “A Library  
161 of Human Electrographic Data and Analyses” Miller (2019) and is available at  
162 <https://searchworks.stanford.edu/view/zk881ps0522>. All patients participated in a purely voluntary  
163 manner, after providing informed written consent, under experimental protocols approved by the  
164 Institutional Review Board of the University of Washington (#12193). All patient data was anonymized  
165 according to IRB protocol, in accordance with HIPAA mandate.

### *Subjects*

166

167 From the above-mentioned library, we included only those subjects that had data in at least two  
168 paradigms in such a way that maximized the number of subjects for pairs of cognitive states (see below).  
169 Cumulatively over the chosen task pairs, the dataset contained 18 human subjects (8 females, 7 males,  
170 and 3 subjects without reported sex information). However, not all subjects had data in all of the 6  
171 cognitive states (median number of states across subjects = 3). Subjects -disregarding 3 with missing age  
172 information- were on average 30.8 years old (+/- std= 9.3). Average number of electrodes per subject  
173 was 53.5 (+/- std=12.7) with an inter-electrode distance of 1cm. Fig. 2 shows the electrode location maps  
174 of all subjects. As shown in Fig. 2, all subjects have electrodes over at least two of the frontal, temporal,  
175 and parietal lobes in either the left or right hemisphere, suggesting coverage of multiple functionally  
176 distinct regions. All data were sampled at 1000Hz, with a built-in 0.15-200 Hz bandpass filter. Beyond  
177 the initial data cleaning performed by Miller et al (2019), including rejection of channels with obvious  
178 artefact or epileptic activity, portions of the data with excessive inter-ictal activity were removed if  
179 necessary.



180

181 *Fig. 2 – Electrode location maps of all subjects. Only electrodes that were clear of obvious artefacts and epileptic activity (cf. Miller*  
 182 *2019) and were shared across conditions (e.g. Rest and Motor) are shown here and were included in the analyses. The nine subjects*  
 183 *at the top half of the figure have left hemispheric electrode coverage, while the other nine subjects have right hemispheric electrode*  
 184 *coverage. In each subject, at least two of the frontal, temporal, and parietal lobes are covered by the electrode grids.*

185 **Experimental Design and Statistical Analysis**

186 *Behavioral paradigms*

187 In order to increase the statistical power of cross-state comparisons of FC, we used those paradigms that  
 188 had the highest number of subjects with highest possible number of independent cognitive states: resting  
 189 state, cue-based motor task, verb generation task, and 2-back task datasets. These tasks represent a  
 190 highly diverse set of cognitive states in terms of cognitive demands. Motor and speech tasks have a pre-  
 191 stimulus interval while the 2-back task employs a continuous block design. As a result, we investigated

192 the intrinsic FC across 6 cognitive states including: resting state (*Rest*), pre-stimulus motor (*Base<sub>Motor</sub>*),  
193 pre-stimulus speech (*Base<sub>Speech</sub>*), post-stimulus motor (*Motor*), post-stimulus speech (*Speech*), and  
194 *2Back*.

195 Resting state (*Rest*): All subjects underwent resting state recordings while fixating on an “X” on the  
196 wall 3 m away, for 2-3 minutes. For more information regarding this data, see (Miller et al. 2009, 2012).

197 Cue-based motor task (*Motor*): seventeen out of the eighteen subjects had motor task data. Patients were  
198 instructed to repetitively flex and extend all fingers based on a visual word cue indicating the body part  
199 that should be moved (an alternative cue in a separate run instructed tongue movements not analyzed in  
200 this study). Movements were self-paced with a rate of ~1-2Hz using the hand contralateral to the side of  
201 the cortical grid placement. Each movement interval was 3s long, preceded by a rest interval of the same  
202 length (blank screen). To maximize independence between trials, we excluded 0.5s from the two tails of  
203 the trials, resulting in a [-2.5, 2.5]s interval relative to cue onset. We analyzed two task states comprising  
204 the pre-stimulus ([-2.5, 0]s) and post-stimulus ([0, 2.5]s) intervals. There were between 30 and 75 trials  
205 of rest and movement per subject. See Miller et al. (2007) for more detailed information of this task.  
206 Miller et al. have reported robust task-related power changes in the high frequency or high gamma range  
207 in all subjects, implying that the subjects have task-appropriate electrode coverage suitable for our study.

208 Verb generation task (*Speech*): Five of the 18 subjects had performed the speech task. The speech data of  
209 one subject was excluded due to mismatching electrode grids with respect to the other tasks. Written  
210 nouns (approximately 2.5 cm high and 8–12 cm wide) were presented on a screen positioned  
211 approximately 1 m from the patient, at the bedside. Patients were asked to speak a verb that was  
212 semantically related to the noun. For example, if the noun read “ball”, the patient might say “kick”, or if  
213 the noun read “bee”, the patient might say “fly”. Between each 1.6-second noun there was a blank-screen  
214 1.6-second interstimulus interval. To avoid overlap between the trials during data analysis, we defined  
215 the trials from -1.5 to 1.5s with respect to stimulus onset. We analyzed two task states comprising the

216 pre-stimulus ([-1.5, 0]s) and post-stimulus ([0, 1.5]s) intervals. Further details of the speech task data are  
217 provided in a prior investigation using these data (Miller et al. 2011).

218 2-back task (*2Back*): Four subjects out of the eighteen had performed the 2back task. Among the  
219 available task conditions (0back, 1back, and 2back), we used 2back since it requires higher cognitive  
220 involvement (e.g. attention and decision making) which warrants larger possible divergence of cognitive  
221 state from resting state and the simple motor task. The stimuli comprised pictures of 50 houses 10 of  
222 which were 2back targets, each presented for 600ms. Subjects were instructed to flex their finger when a  
223 picture was the same as the one presented two trials earlier (i.e. target). For more details see (Miller  
224 2019). Note that because the Nback task consists of a continuous stream of pictures, we considered task  
225 engagement to be continuous. Thus, in the FC estimations of 2Back, we analyze this data exactly same  
226 as the resting state data after concatenating all respective blocks (see “Static functional connectivity” in  
227 “Materials and Methods”).

#### 228 *Data preprocessing*

229 The publicly available data were initially cleaned (Miller 2019). However, visual inspection of the signal  
230 timecourses indicated the need for further cleaning in two subjects. Brief periods of epileptiform activity  
231 where thus manually marked and removed from the data of those subjects. Line noise was removed  
232 using two 60 Hz and 120 Hz 2nd order Butterworth notch filters. To remove low frequency drift and  
233 high frequency noise, data were filtered by low-pass (120 Hz cutoff) and high-pass (2 Hz) 4th order  
234 Butterworth filters. For task data, stimulus-locked trials were based on the pre- and post-stimulus  
235 intervals described above. All data analyses were implemented in MATLAB, using FieldTrip  
236 (Oostenveld et al. 2011) and custom codes that can be found here:  
237 [https://github.com/connectlab/IntrinsicFC\\_Mostame](https://github.com/connectlab/IntrinsicFC_Mostame).

238 Our results primarily focus on phase coupling. Corresponding results for amplitude coupling are also  
239 provided in a more compact fashion in the corresponding sections. Phase- and amplitude-coupling are  
240 directly compared in section “Stability of spatial organization across phase- and amplitude coupling”

241 (Fig. 6). We estimated FC across five canonical frequency bands including: theta (5-7 Hz), alpha (8-13  
 242 Hz), beta (14-30 Hz), gamma (31-60 Hz), and high gamma (61-110 Hz). The delta band (~1-4Hz) was  
 243 not included since the relatively short trial periods didn't permit its reliable estimation from few  
 244 oscillation cycles. We note that the use of canonical bands offers only a rough delineation of oscillatory  
 245 processes, and separating the latter from broadband processes and defining them on an individual basis  
 246 may provide refined results in the future. Below, static and dynamic estimation of phase- and amplitude-  
 247 coupling are described.

#### 248 *Static functional connectivity*

249 Static FC was estimated in a single time window for pre-stimulus (*Base<sub>Motor</sub>* and *Base<sub>Speech</sub>*) and post-  
 250 stimulus intervals (*Motor* and *Speech*). Static FC was assessed in terms of phase coupling using the  
 251 phase locking value (PLV)(Lachaux et al. 1999):

$$PLV(f) = \frac{1}{N} \left| \sum_{n=1}^N e^{j\Delta\phi_i(f)} \right|$$

252 where  $f$  is frequency,  $N$  is number of trials, and  $\Delta\phi_n$  is the phase difference between the corresponding  
 253 frequency components of the two electrode signals in trial  $n$ .

254 To derive amplitude coupling, the envelopes of pairwise band-limited signals (estimated through Hilbert  
 255 transform) were correlated. Subsequently, temporal correlation values of all trials were averaged to  
 256 obtain a single value for each electrode pair (ranging from -1 to 1), over the corresponding frequency  
 257 band. To facilitate comparison with PLV, which ranges from 0 to 1, absolute values of amplitude  
 258 coupling were used:

$$Amplitude\_coupling(f) = \frac{1}{N} \left| \sum_{n=1}^N corr(env(x_{1,n}^f), env(x_{2,n}^f)) \right|$$

259 Where  $f$  is frequency,  $N$  is number of trials,  $corr()$  is Pearson correlation,  $env()$  is signal envelope driven  
 260 from Hilbert analysis, and  $x_{i,n}^f$  is frequency-specific component of  $i^{\text{th}}$  electrode signal ( $i = 1, 2$ ) on the  $n^{\text{th}}$   
 261 trial.

262 Static FC for the continuous conditions *Rest* and *2Back* was estimated by averaging the dynamic FC (as  
 263 defined below) over time.

#### 264 *Dynamic functional connectivity*

265 Dynamic FC was used to dissociate broad-band versus independent band-limited contributions to the  
 266 dynamics of the intrinsic FC architecture. Windows were shifted every 1sec, and window length varied  
 267 as a function of canonical frequency band (75, 100, 200, 400, and 800 cycles for theta, alpha, beta,  
 268 gamma, and high gamma frequency bands, respectively). Dynamic amplitude coupling was estimated as  
 269 described in the static framework for each time window, when  $N$  is equal to 1. However, dynamic phase  
 270 coupling was estimated using an alternate method.

271 In contrast to task-based phase coupling, commonly estimated as phase-lag consistency over trials  
 272 (Lachaux et al. 1999), *continuous* phase coupling was estimated as phase-lag consistency over time  
 273 (Mostame and Sadaghiani 2020; Sadaghiani et al. 2012). The above-defined PLV measure adjusted to  
 274 continuous data is defined as:

$$PLV_{Rest}(f) = \frac{1}{M} \left| \sum_{m=1}^M e^{j\Delta\phi_m(f)} \right|$$

275 Where  $M$  is the number of time samples within the time window.

#### 276 *Presence of intrinsic architecture*

277 To assess whether FC organization is stable across cognitive states (Fig. 1; scenarios II, IV vs. I, III),  
 278 spatial Pearson correlations were calculated for each state pair. Cross-state correlations were tested  
 279 against a null model that spatially permuted one of the matrices 500 times ( $q < 0.05$ ; Benjamini-Hochberg  
 280 FDR corrected for number of subjects  $\times$  frequencies  $\times$  task states). Specifically, the phase of the 2D

281 Fourier transform of the matrix was shuffled while keeping the amplitude intact. The odd symmetry of  
282 phases was preserved over frequencies in the 2D domain. The matrix was reconstructed using the inverse  
283 2D Fourier transform, and its spatial correlation with the other matrix (which was not shuffled) assessed  
284 (Prichard and Theiler 1994; Tewarie et al. 2016; Wirsich et al. 2017).

285 To determine the effect size of cross-state correlations, spatial stability of FC within *Rest* was estimated  
286 for comparison. *Rest* data of each subject was divided into two parts of equal length, and the similarity  
287 (2D Pearson correlation) between the static matrices of the two parts was calculated (see Fig. 3).

#### 288 *Shared intrinsic architecture across frequency bands*

289 To assess whether FC in different oscillation frequencies share a similar intrinsic architecture (Fig. 1;  
290 scenarios III, IV vs. I, II), spatial similarity between the static FC organization of all pairs of frequency  
291 bands was calculated. Since the intrinsic architecture is by definition considered stable across cognitive  
292 states (Cole et al. 2014; Petersen and Sporns 2015), we estimated such an intrinsic organization for each  
293 frequency band by taking the geometrical mean of its static FC organization over all cognitive states  
294 (*Rest*, *Base<sub>Motor</sub>*, *Base<sub>Speech</sub>*, *Motor*, *Speech*, and *2Back*). Then, we calculated spatial correlation of this  
295 ‘frequency-specific’ intrinsic architecture over every pair of frequency bands (Fig. 4).

#### 296 *Broadband vs. band-limited coupling events*

297 Spatial correlation of FC organization across frequency bands may be driven by multiple band-limited  
298 processes with a similar spatial organization or, alternatively, a single broadband process. To dissociate  
299 between these scenarios, we compared FC timecourses of different frequency bands. The procedure was  
300 applied only to the resting state data due to limited length of trial-based task data. To focus on the  
301 frequency-invariant connections, only the top 25% strongest connections among all cross-state  
302 geometrical mean FC matrices of all bands were considered (mean connectivity strength  $\pm$  std= 0.60  $\pm$   
303 0.13 pooled over all connections and frequency bands and averaged over subjects). Within the selected  
304 connections, temporal correlations between phase coupling timecourses (see “Dynamic functional

305 connectivity” in “Materials and Methods”) were estimated over pairs of different bands. Finally, for each  
306 subject and frequency pair, all temporal correlations were pooled over connections (shown in Fig. 5).

307 To test to what degree the FC dynamics of two bands are systematically correlated, we generated a set of  
308 500 surrogate data by phase-permuting the FC timecourse of one of the frequency bands (for each  
309 frequency pair and subject). For each permutation, we extracted the histogram of temporal correlations  
310 across all electrode pairs between the original and phase-permuted FC dynamics. The 500 surrogate  
311 histograms were pooled into a single histogram for each subject and frequency pair (Fig. 5). To assess if  
312 the original histogram was different from the surrogate histogram (indicating systematic correlation  
313 between frequency bands in the original data), we compared their mean, std, and skewness ( $q < 0.05$ ;  
314 FDR-corrected for all subjects, pairs of frequency bands, and three histogram measures).

#### 315 *Shared intrinsic architecture across connectivity measures*

316 To directly assess the spatial similarity of intrinsic FC organization across phase- and amplitude coupling  
317 as well as over all frequencies and cognitive states, we estimated spatial Pearson correlation between all  
318 possible pairs of FC matrices (across FC measures, cognitive states, and frequency). Finally, we  
319 averaged the resulting value of each pair-wise comparison across all subjects (Fig. 6; upper diagonal).  
320 We tested the significance of each bin by using the same 2D permutation method described above,  
321 phase-permuting one of the two matrices 500 times ( $q < 0.05$ ; FDR corrected by Benjamini-Hochberg  
322 method).

#### 323 *Addressing source leakage*

324 Source leakage refers to the simultaneous detection of a particular brain signal (as a source) at several  
325 sensors due to volume conduction (Schoffelen and Gross 2009), which may generate spurious  
326 connectivity between electrode pairs especially in neurophysiological scalp recordings like EEG and  
327 MEG (J. M. Palva et al. 2018). Although much less of a concern for ECoG, we tested whether our results  
328 are affected by this potential confound.

329 First, following equivalent procedures for task and rest conditions as described for PLV, we employed  
330 imaginary part of coherency (ImC; introduced by Nolte (2004)). ImC is the most commonly used  
331 measure suppressing zero-lag connectivity. This common approach rests on the assumption that  
332 electricity spreads quasi-instantaneously, but comes at the cost of also removing real zero-lag  
333 connectivity (M. X. Cohen 2015). Therefore, as a second approach, we regressed out electrode distance  
334 dependencies from FC values. Given the fact that volume conduction is dependent on electrode distance  
335 (Dubey and Ray 2019; Rogers et al. 2019; Rouse et al. 2016), this approach is expected to substantially  
336 dampen possible volume conduction effects. Specifically, we fit cubic spline curves to the mean of the  
337 FC values within each non-overlapping 1cm range of electrode distance. We subtracted the value of the  
338 fitted curve from all corresponding FC values. This procedure removes any collinearity between the two  
339 measures resulting from their dependence on electrode distance. Once zero-lag FC or distance  
340 dependencies were removed, we estimated the cross-state spatial correlations as in section “Source  
341 leakage contributions” (Fig. 7).

## 342 Results

343 FC matrices were extracted for all subjects, cognitive states, and canonical frequency bands. First, to  
344 establish the presence of a cognitive state-invariant, i.e. intrinsic, FC organization, spatial correlation of  
345 the FC matrix across *Rest* and the three active task processing states (e.g. *Motor*) were assessed within  
346 each frequency band. Subsequently, the intrinsic FC organization most representative of each frequency  
347 was defined as the (geometric) mean of FC matrices across all six cognitive states in that frequency.  
348 Next, this representative organization was spatially compared across all bands to quantify frequency-  
349 invariance of FC organization. Then, we compared FC timecourses across frequency bands to address  
350 whether the spatial frequency-invariance indeed reflects band-limited coupling in temporally  
351 independent frequencies or, alternatively, a broadband coupling phenomenon. Finally, to identify the  
352 most likely scenario from the four hypothetical scenarios illustrated in Fig. 1, the spatial similarity across  
353 all pairs of FC matrices for all cognitive states and frequency bands was assessed.

## 354 A state-invariant intrinsic FC organization

355 *Cross-state spatial correspondence in real vs. surrogate data*

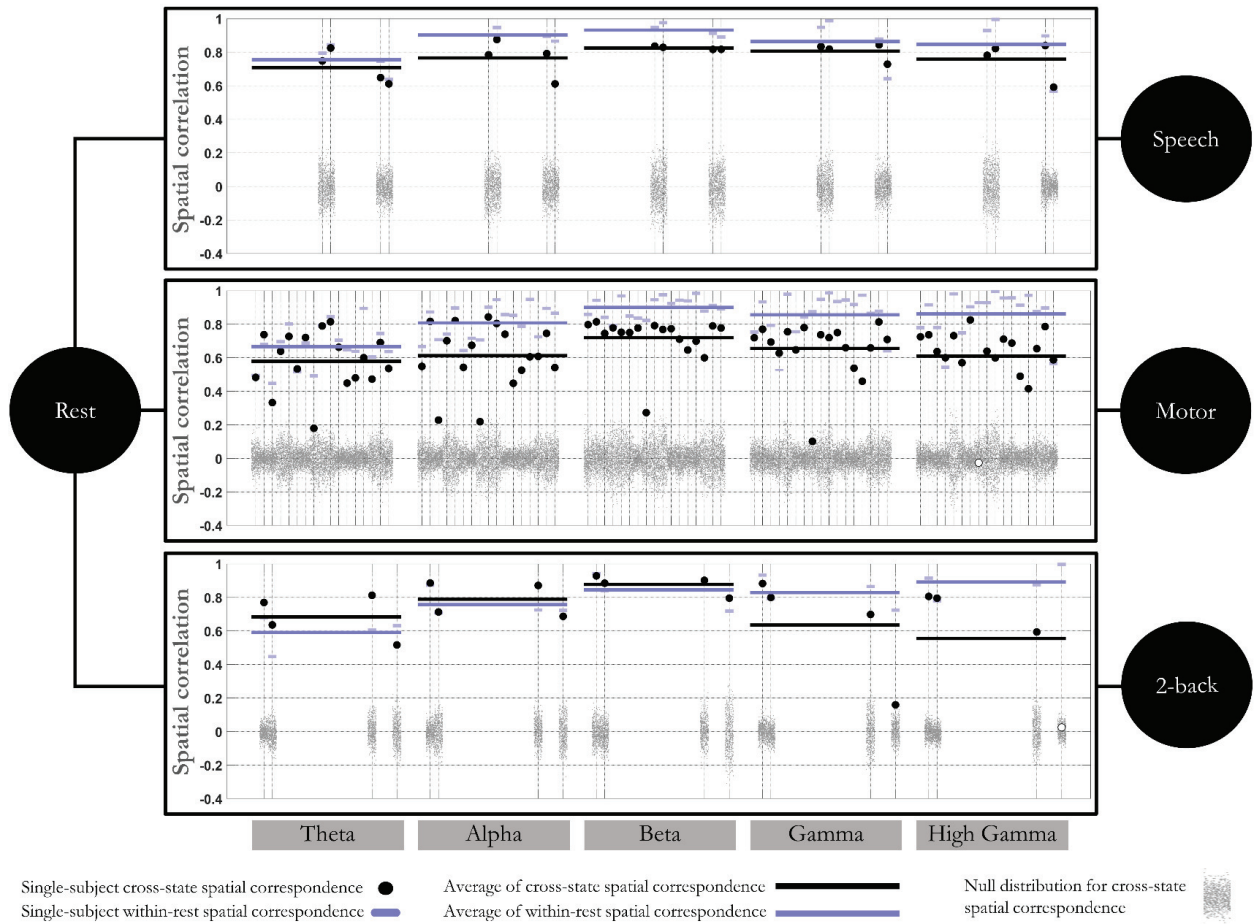
356 Spatial correlations between FC matrices of *Rest* and the three active task processing states were  
357 assessed in every frequency band (Fig. 3; black circles). All three pairs of cognitive states demonstrated  
358 strong spatial similarity in all frequencies (average  $r = 0.67$ ;  $\text{std} = 0.18$ ). Spatial correlations were  
359 compared to surrogate correlations generated after spatially shuffling one of the two matrices in 2D  
360 Fourier space (500 permutations; Fig. 3; Gray dot clouds). At the group level, we compared the subject-  
361 specific cross-state correlations (averaged over all cross-state conditions) with the mean value of the  
362 corresponding null models (averaged over permutations and all cross-state conditions). For all frequency  
363 bands, cross-state spatial similarity exceeded the respective null model (paired  $t$ -test significant at  $q <$   
364  $0.05$  with FDR correction, listed for theta through high gamma in ascending frequency:  $t_{17}=3.90$ ;  
365  $p<0.005$ ;  $t_{17}=3.86$ ;  $p<0.005$ ;  $t_{17}=5.81$ ;  $p<0.005$ ;  $t_{17}=3.06$ ;  $p<0.005$ ;  $t_{17}=2.45$ ;  $p<0.05$ ). At the individual  
366 level, the spatial similarity across cognitive states exceeded chance level for all individual subjects and  
367 frequency bands with only 2 exceptions out of 125 cross-state cases shown in Fig. 3 ( $q<0.05$ ; Benjamini-  
368 Hochberg corrected for subjects  $\times$  frequencies  $\times$  cognitive state pairs). This outcome indicates the  
369 presence of an intrinsic FC organization of phase coupling in all frequency bands. Results for amplitude  
370 coupling were comparable ( $r = 0.45 \pm 0.22$  averaged across subjects, frequency bands and *Rest-Motor*,  
371 *Rest-Speech*, and *Rest-2Back* condition pairs).

372 *Cross-state vs. within-state spatial correspondence*

373 Spatial similarity of FC patterns was also assessed *within* a single cognitive state for comparison. The  
374 relatively long duration of resting state recordings allowed comparing time-averaged FC matrices from  
375 two equal halves of the run (Fig. 3; purple data points). Overall, spatial similarity *within* resting state was  
376 either equivalent or only slightly stronger compared to the similarity *across* cognitive states.  
377 Specifically, the average reduction of the  $r$  values over all cross-state conditions and frequency bands  
378 was  $11 \pm 12\%$  (Mean  $\pm$  std). Therefore, divergence of spatial organization of FC across different

379 cognitive states is comparably small. Amplitude coupling showed comparable albeit slightly larger  
 380 reduction values (Mean  $\pm$  std:  $0.17 \pm 0.16$ ).

381



382

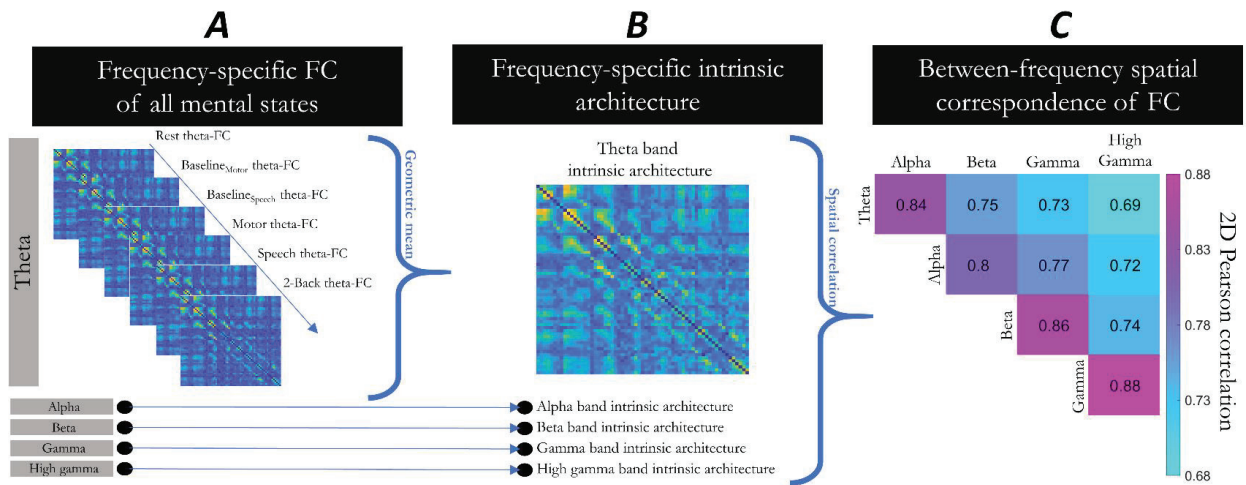
383 *Fig. 3 – Example of spatial correspondence between FC matrices over three pairs of rest vs task states. States include task-free*  
 384 *resting-state (“Rest”), verb generation (“Speech”), cue-based finger flexing (“Motor”), and memory recall (“2Back”). Not all*  
 385 *subjects had data in all these states. In each subplot, frequency band is on the x-axis and spatial correlation on the y-axis. In each*  
 386 *column of the plots, black dots correspond to the cross-state correlation of each subject (long horizontal black line represents*  
 387 *average across subjects). short horizontal purple lines represent the within resting-state correlations of FC organization in each*  
 388 *subject (long horizontal purple line shows average across subjects). The order of subjects is preserved across subplots to allow*  
 389 *subject-specific comparison between cross-state pairs. Gray dot clouds represent the null model for the corresponding subject,*  
 390 *frequency band, and cross-state pairing. The null model was generated by randomly permuting one of the matrices in 2D Fourier*

391 *space. Pair-wise correlations significantly exceed the null model in the vast majority of individual subjects and frequency bands (2*  
392 *exceptions out of the 125 pairs shown here), supporting the presence of a stable intrinsic FC organization.*

### 393 Intrinsic FC organization shared across frequency bands

394 Above, we showed the presence of an intrinsic FC organization that is stable across cognitive states  
395 within each of the canonical frequency bands (Fig. 3). Is a unifying state-invariant FC organization  
396 shared across frequency bands, or does each specific frequency have its own unique spatial organization?  
397 Here, we assess how the state-invariant FC organization of each frequency band spatially correlates with  
398 that of other bands. To this end, for each subject and frequency band, we calculated the geometric mean  
399 of the FC matrices from all six cognitive states as the representative intrinsic organization of that  
400 frequency band (Figure 4. A & B). The geometric mean is often used to find the central tendency for  
401 different items, emphasizing consistency. In other words, if an electrode pair has a small FC value in  
402 even a single cognitive state, that pair obtains a small value in the intrinsic organization matrix since it is  
403 not consistent over all cognitive states.

404 For each subject, we assessed spatial correlations across pairs of representative (mean) intrinsic FC. For  
405 each pair of frequencies, we statistically tested the significance of FC similarity using the spatial  
406 permutation method described above(500 permutations). At the group level, we found significantly  
407 higher cross-frequency similarity of FC organization compared to null data (pair-wise *t*-test against the  
408 mean correlation from permutations; all  $t_{17} > 9.37$ ,  $p < 2e-8$ ). At the individual level, the cross-frequency  
409 spatial similarity exceeded chance level of the null model for all frequency pairs and all subjects  
410 ( $q < 0.05$ ; FDR corrected for  $18 * C \binom{5}{2} = 180$  cases of subjects  $\times$  frequency pairs). Figure 4C shows the  
411 spatial correlation values averaged over subjects (upper triangle) as well as the number of subjects  
412 showing a significant effect (lower triangle). The strong spatial relationship ( $r = 0.69$  to  $0.88$ ) across all  
413 frequency pairs demonstrates that FC is governed by a universal spatial organization largely shared  
414 across frequency bands. Equivalent results from amplitude coupling were observed ( $r = 0.45$  to  $0.61$ ).



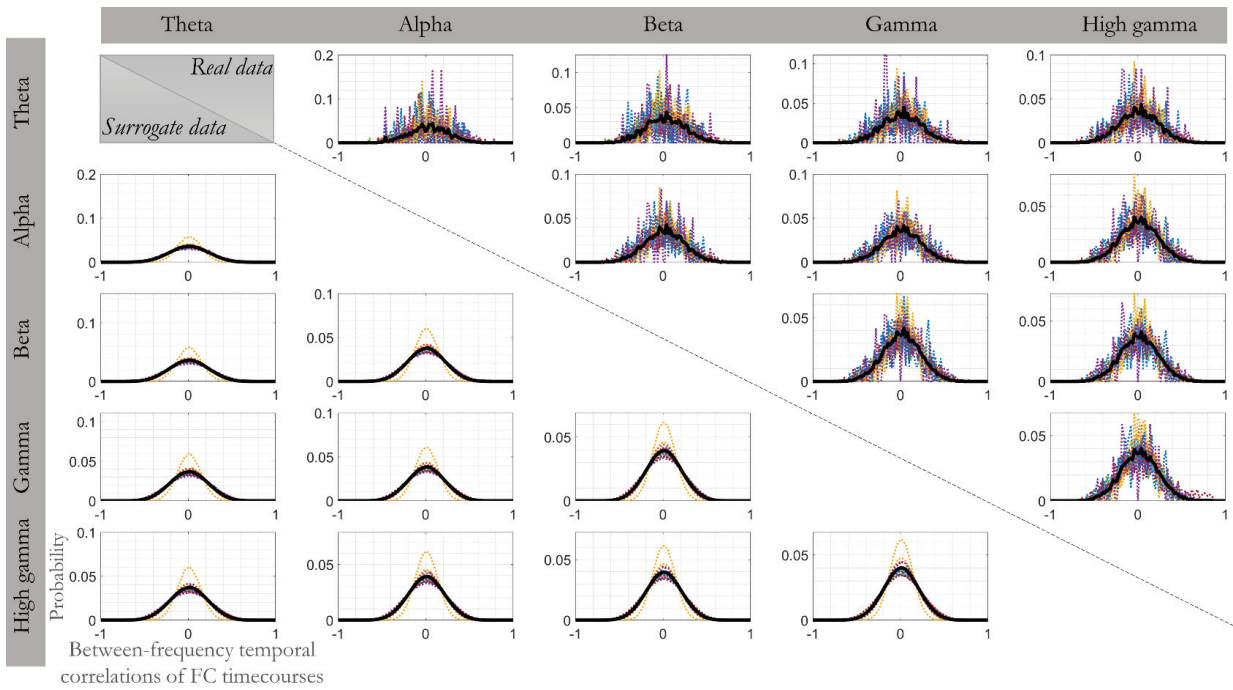
415

416 *Fig. 4 – Spatial similarity of intrinsic FC organization across frequency bands. Panels A-B illustrate the approach. A) Schematic*  
 417 *example of FC matrices from all cognitive states available for a given subject shown for the theta band. B) State-invariant*  
 418 *representation of intrinsic FC organization of theta band was calculated by taking the geometric mean of the theta band FC matrices*  
 419 *shown in A. For each subject, such frequency-specific intrinsic architecture was separately extracted for each frequency. The*  
 420 *ensuing frequency-specific intrinsic organization entered spatial correlation analysis across pairs of frequency bands. Panel C)*  
 421 *depicts the between-frequency spatial correlation values averaged across all subjects. Rows/columns indicate frequency bands from*  
 422 *theta to high gamma. Correlation values of all frequency pairs were statistically significant across all individual subjects. The high*  
 423 *correlation values ( $r > 0.69$ ) indicate the presence of an intrinsic organization that is spatially similar across frequency bands.*

#### 424 Temporal dynamics dissociating broadband vs. band-limited FC

425 Our observation that the intrinsic FC organization is highly similar across frequency bands may be  
 426 explained by one of two alternative scenarios. Either temporally independent coupling processes in  
 427 multiple frequency bands indeed share a unifying spatial organization, or a single broadband coupling  
 428 process (e.g. coupled bursts with sharp on/offset) underlies FC in all frequencies. In the latter case, FC  
 429 would be temporally correlated over frequencies. To dissociate between the two scenarios, we inspected  
 430 temporal correlations between connection-wise FC time courses of different frequency bands within the  
 431 resting state condition because it provides the most data of all cognitive states (2-3 minutes). We only  
 432 focused on those connections of the intrinsic FC organization that were strong in all frequency bands  
 433 (top 25% of the representative mean organization illustrated in Fig. 4B; mean FC= 0.60; std= 0.13;

434 averaged over subjects). This approach ensured that we only included electrode pairs involved in the  
 435 task-invariant FC organization of all bands. As shown in Fig. 5 (top subplots above the diagonal; 'real  
 436 data'), we detected a symmetric histogram of temporal correlation values centered on zero for every  
 437 subject and pair of frequency bands. The lower subplots below the diagonal of Fig. 5 show an equivalent  
 438 temporal correlation analysis for surrogate data generated by temporally permuting phases of one of the  
 439 FC dynamics in Fourier space (500 permutations). The distribution of temporal correlations was highly  
 440 similar to the corresponding histogram of the real data. Again, similar results were obtained for  
 441 amplitude coupling.



442  
 443 *Fig. 5 – Histogram of temporal correlation values between resting state FC dynamics of different frequency bands for real (upper*  
 444 *diagonal) and surrogate (lower diagonal; pooled over 500 repetitions) data. The surrogate data represent temporally phase*  
 445 *permuted and thus temporally independent FC time courses. Each panel corresponds to a specific pair of frequency band as labeled.*  
 446 *In each panel, histograms averaged over subjects are shown as thick black lines, while single-subject histograms are shown as*  
 447 *narrow dotted lines of different colors. The x-axis indicates temporal Pearson correlation values of FC dynamics of the two*  
 448 *frequency bands, and the y-axis shows the probability of observing the respective values over electrode pairs. The histograms for*  
 449 *real data were zero-centered and symmetric as were those observed for the simulated temporally independent FC dynamics. This*

450 *observation is consistent with the presence of multiple frequency-specific processes with temporally independent time-varying*  
451 *dynamics rather than a single broadband phenomenon.*

452 To test for an overall tendency towards positive or negative correlations between FC temporal dynamics  
453 of each frequency pair, we compared mean, std, and skewness between histograms of the real and null  
454 data. The (grand average) difference in the three measures between histograms of the real and null data  
455 (averaged across repetitions) were 0.01, 0.01, and 0.02 ( $\pm$ std= 0.03, 0.01, and 0.13), respectively. All  
456 differences were negligible in size, suggesting the absence of a broadband process. Moreover, a large  
457 proportion of all cases (all subjects, pairs of frequency bands, and the three histogram measures) did not  
458 pass the significance test when compared to surrogate data (73, 68, and 95% of all cases for mean, std,  
459 and skewness differences, respectively;  $q < 0.05$ ). This observation implies that FC fluctuations in  
460 different frequency bands do not temporally coincide (in a linear sense) more frequently than expected  
461 by chance. We conclude that the observed spatial concordance of FC organization across frequencies is  
462 not generated by a single broadband phenomenon, but rather reflects multiple frequency-specific  
463 coupling processes unfolding within the same universal spatial organization.

## 464 Stability of spatial organization across phase- and amplitude coupling

465 In previous sections, we separately tested the stability of FC organization across cognitive states and  
466 frequency bands. Next, in order to test the four scenarios presented in Fig. 1, we assessed the stability of  
467 FC organization across all possible pairs of cognitive states and frequency bands. We further extended  
468 this comprehensive approach to a comparison across different modes of connectivity, i.e. phase- and  
469 amplitude coupling.

### 470 *Spatial organization of phase-coupling*

471 We estimated spatial correlation for all possible pairs of FC matrices across cognitive states and  
472 frequencies for each subject separately, resulting in a *correspondence lattice* (Fig. 6A). For visualization  
473 purposes, the upper triangle of the correspondence lattice in Fig. 6A shows the correspondence lattice  
474 averaged over all subjects ( $r = 0.57 \pm 0.18$  including cross-frequency comparisons;  $r = 0.69 \pm 0.18$  for

475 within-frequency comparisons only). Using the same spatial permutation test that was used for previous  
476 sections, we tested the significance of each bin of the correspondence lattice for each subject. The lower  
477 triangle of Fig. 6A reports the proportion of subjects passing significance threshold for each comparison  
478 ( $R=500$ ;  $q<0.05$ ; Benjamini-Hochberg FDR corrected for all cases of subjects  $\times$  pairs of cognitive state  $\times$   
479 frequency bands). We observed evidence for spatial similarity across all pairs of FC matrices in overall  
480 99.3% of the single-subject comparisons, strongly supporting hypothesis IV (cf. Fig. 1). This outcome  
481 shows that the spatial FC organization is to a large degree consistent across all cognitive states and  
482 frequency bands.

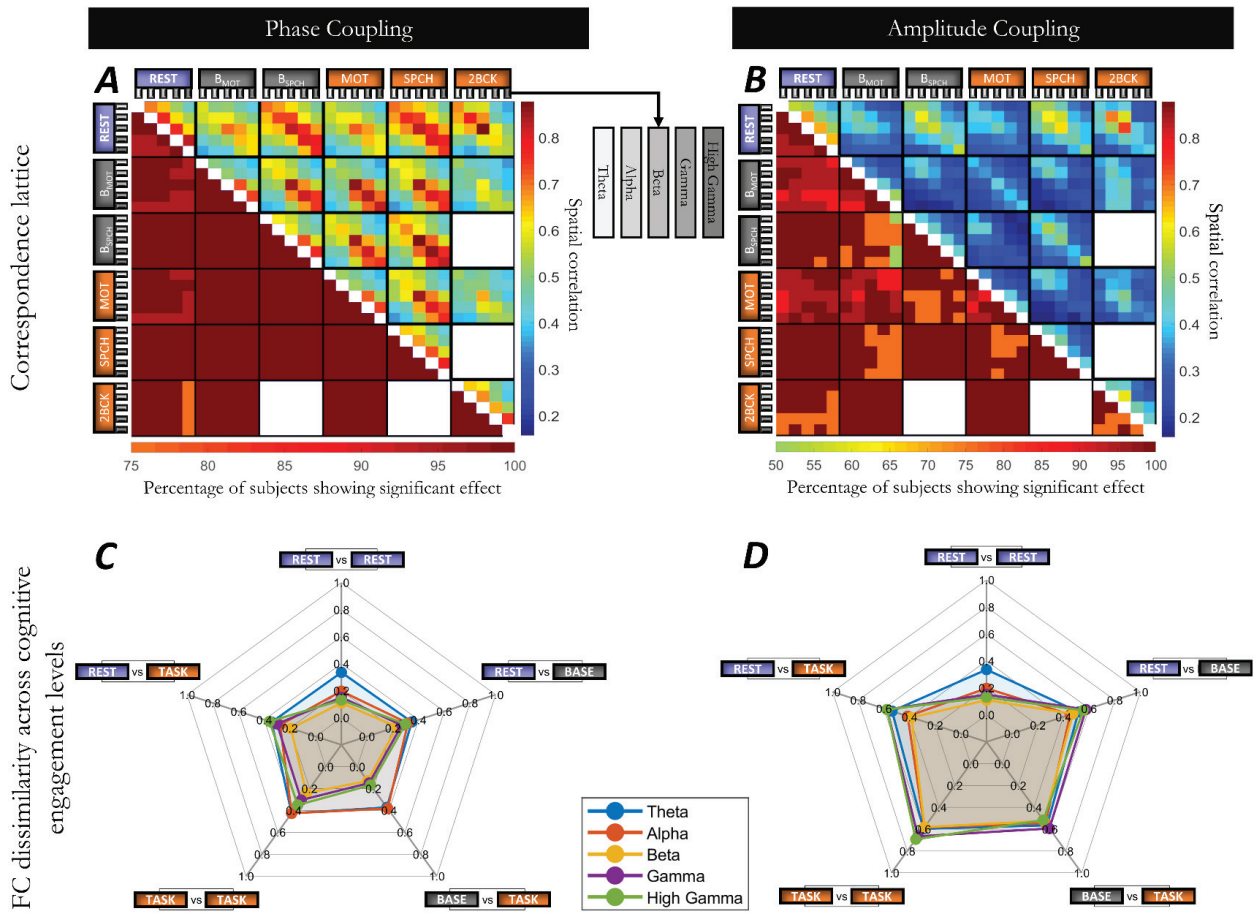
483 We further summarized information from the correspondence lattice according to cognitive engagement  
484 levels (Fig. 6C). These levels are conceptualized to gradually increase from task-free resting state (*Rest*),  
485 to pre-stimulus baseline involving task-set maintenance (*Base<sub>Motor</sub>* and *Base<sub>Speech</sub>*), to active processing  
486 during stimulation and motor output (*Motor*, *Speech*, and *2Back*). We focused on the amount of FC  
487 dissimilarity ( $1-r$ ) across pairs of cognitive engagement levels in order to emphasize the change in FC  
488 organization. In all frequency bands the radar plots approached a circle, showing that the dissimilarity of  
489 FC was of comparable magnitude across all level pairs. In other words, more distant pairs of engagement  
490 levels, most notably base-task and task-task contrasts as commonly applied in electrophysiological  
491 studies, were no more dissimilar than the closer rest-rest pair.

#### 492 *Spatial organization of amplitude-coupling*

493 Amplitude coupling is a distinct mode of oscillation-based FC beyond phase, likewise subserving long-  
494 range neural communication and cognitive processes (Engel et al. 2013). We have previously  
495 hypothesized that FC organization in both modes entails an intrinsic, task-independent component  
496 (Mostame and Sadaghiani 2020). Therefore, we asked whether the same observation, i.e. consistency  
497 across cognitive states and frequency bands, also holds true for amplitude coupling. We extracted FC  
498 matrices of all cognitive states and frequency bands using amplitude coupling as connectivity measure.  
499 Fig. 6B visualizes the outcome for amplitude coupling (equivalent to Fig. 6A for phase coupling). Spatial

500 correlation values were moderate to strong (average of upper triangle of 6B  $r= 0.42 \pm 0.21$ ). Importantly,  
 501 as shown in the lower triangle of 6B, spatial correlation of FC matrices across all cognitive states and  
 502 frequencies were significant in overall 94.7% of the comparisons ( $q<0.05$ ; Benjamini-Hochberg FDR  
 503 corrected for subjects  $\times$  pairs of cognitive state  $\times$  frequency bands), in line with hypothesis IV in Fig. 1.  
 504 In the radar plots for amplitude coupling (Fig. 6D) FC dissimilarity between more distant pairs of  
 505 cognitive engagement levels were only marginally larger in magnitude compared to the rest-rest pair. We  
 506 conclude that the intrinsic architecture is also consistent across cognitive states and frequency bands for  
 507 amplitude coupling.

508



509

510 Fig. 6– Spatial correlation between FC matrices from all possible pairs of cognitive states and frequency bands for phase coupling  
 511 and amplitude coupling. A-B) In the correspondence lattice, axes labels correspond to cognitive states (“MOT”: Motor; “SPCH”:  
 512 Speech; “2BCK”: 2Back; “B<sub>MOT</sub>”: Base<sub>Motor</sub>, and “B<sub>SPCH</sub>”: Base<sub>Speech</sub>) and frequency bands (theta to high gamma). Upper triangles  
 513 show correlation values averaged across all subjects, with effect size indicated by color (vertical color bar). For each subject, a set  
 514 of 500 surrogate data were generated to test the significance of the correlation values. The number of subjects showing significance  
 515 in each bin of the correspondence lattice is presented in the lower triangles (horizontal color bar). The lower triangles in A and B  
 516 conform with hypothesis IV in Fig. 1. C-D) The radar plots show the magnitude of FC dissimilarity ( $1 - r$ ) across all levels of  
 517 cognitive engagement. Cognitive engagement is conceptualized to gradually increase from resting state: (“Rest”) to inter-trial  
 518 baseline periods during paradigms (“Base”, averaged over Base<sub>Motor</sub> and Base<sub>Speech</sub>), to active processing (“Task”, averaged over  
 519 Motor, Speech and 2Back). Radar plots in different colors correspond to different frequency bands. The comparable magnitude of  
 520 dissimilarity across all pairs of cognitive engagement levels speaks to the presence of an intrinsic spatial organization for both  
 521 phase- and amplitude coupling.

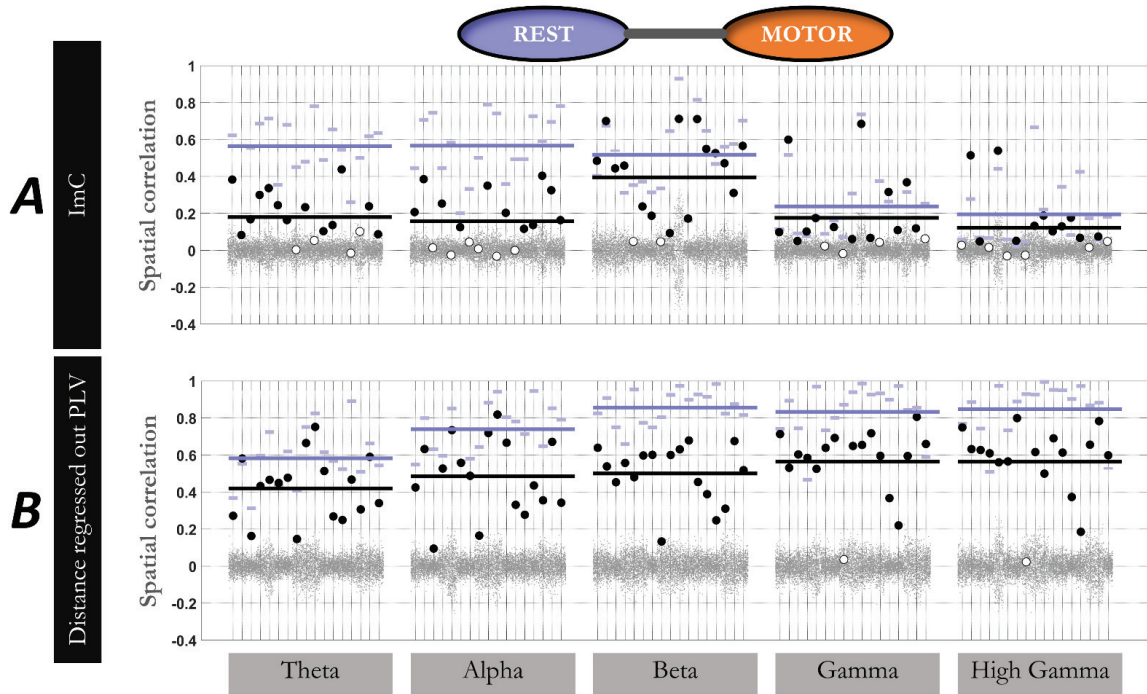
522 *Comparing spatial organization between phase- and amplitude-coupling*

523 We observed differences between phase- and amplitude coupling. While spatial correlation values for  
 524 both were significant compared to their respective null models, values were overall slightly higher for  
 525 phase coupling (Fig. 6A) than for amplitude coupling (Fig. 6B). Further, as the frequency increased,  
 526 within-frequency cross-state correlation values increased for phase coupling (diagonals of small squares  
 527 in Fig. 6A & Fig. 6C), while they slightly decreased for amplitude coupling (Fig. 6B & D). This means  
 528 that task-specific FC changes in phase coupling are more pronounced in lower frequencies (mostly in  
 529 alpha band), resulting in lower cross-state correlations. By contrast, such task-specific changes are  
 530 generally stronger in higher frequencies for amplitude coupling. Collectively, these observations suggest  
 531 the presence of an intrinsic architecture in both phase- and amplitude coupling, but with nuanced  
 532 differences.

533 **Source leakage contributions**

534 Compared to EEG and MEG, ECoG recordings are much less likely to suffer from volume conduction  
 535 especially at the scale of  $\sim >1\text{cm}$  inter-electrode distance (Dubey and Ray 2019). Nevertheless, to  
 536 ascertain that FC stability across cognitive states is largely independent of volume conduction, we

537 replicated our results following suppression of zero-lag connectivity (since electricity spreads quasi-  
 538 instantaneously) and distance dependence of connectivity (since volume conduction is dependent on  
 539 physical distance). We used the *Rest-to-Motor* comparison due to its large number of subjects (See Fig.  
 540 7).



541  
 542 *Fig. 7 - Addressing potential contribution of volume conduction to the cross-state spatial correlation of FC. Rest-to-Motor cross-*  
 543 *state FC correlations based on A) ImC measure, and B) PLV measure after regressing out electrode distance. Each subplot is*  
 544 *organized according to configurations of Fig. 3. A large proportion of data shows the presence of cross-state FC correlations even*  
 545 *after removing possible volume conduction effects, using the two different approaches. This observation suggests that our major*  
 546 *findings are not heavily driven by volume conduction.*

547 *FC measures suppressing zero-lag connectivity (ImC measure)*

548 We found that significant *Rest-to-Motor* cross-state FC correspondence persisted in the majority of  
 549 bands and subjects (63 cases out of 85; with a minimum of 11 out of 17 subjects in each band) even after  
 550 reducing the data to nonzero-lag connectivity (Fig. 7A; FDR-corrected at  $q < 0.05$ ). Despite a reduction in  
 551 effect size likely due to concomitant removal of veridical zero-lag connectivity, the persistence of effects

552 implies that cross-state FC correspondence is not primarily explained by volume conduction effects.  
553 Note that overall relatively low within-*Rest* correlation values of FC matrices (long purple lines in Fig.  
554 7A;  $\sim r = 0.4$ ) speak to low sensitivity of the ImC and the underestimation of the cross-state correlations.

#### 555 *Regressing out distance dependencies from FC*

556 In 83 out of 85 subject-by-frequency cases, spatial organization of FC remained significantly correlated  
557 between *Rest* and *Motor* conditions after removing distance dependencies (Fig. 7B). The large  
558 proportion of significant effects even after removal of a substantial part of connectivity indicates that our  
559 major findings are not primarily driven by distance dependencies. This persistence suggests that volume  
560 conduction contributes no more than a small proportion of the observed consistency of FC organization  
561 across cognitive states and frequency bands.

## 562 **Discussion**

563 The present study sought to answer whether fast oscillatory coupling was sensitive to cognitive context,  
564 or, conversely, associated with a single, state-invariant spatial organization across cognitive domains.  
565 We used ECoG signals of presurgical patients during rest, pre-stimulus intervals corresponding to  
566 maintenance of task-set and attention, and active processing. Across all subjects and all canonical  
567 frequency bands, oscillation-based FC spatial organization changed only slightly in response to cognitive  
568 state. Moreover, the observed spatial organization was largely similar across all frequency bands.  
569 Despite this between-frequency spatial similarity, temporally independent dynamics were detected  
570 across frequency bands speaking against a broadband phenomenon. Taken together, we observed  
571 cognitive state-invariance and frequency-invariance of the distributed FC spatial organization on the one  
572 hand, and frequency-specific FC dynamics at the connection level on the other.

573 To illustrate the concurrent presence of these properties, we consider the analogy of vehicle traffic. In  
574 this analogy, the distributed spatial FC organization corresponds to the pattern of roads, and dynamic FC  
575 corresponds to traffic unfolding on the roads. Our result of state-invariance of the spatial organization  
576 can be conceptualized as the stability of the roads' network pattern irrespective of the ambient conditions

577 such as weather. Illustrating the frequency-invariance of FC spatial organization, different frequency  
578 bands correspond to individual lanes within the same road layout. The absence of linear dependence of  
579 FC dynamics across bands then corresponds to cars travelling in a temporally largely independent  
580 manner on the distinct lanes of the same roads. This analogy highlights how our results extend the  
581 neurobiological understanding of functional networks through the concurrent consideration of distributed  
582 spatial organization and temporal dynamics of FC.

### 583 Stability of oscillation-based FC across cognitive states

584 Spatial stability of fast oscillation-based FC over cognitive states is in strong agreement with prior  
585 observations in fMRI-based FC at infraslow temporal scales. Several neuroimaging studies have shown  
586 that the spatial organization of FC remains largely stable across cognitive states (Cole et al. 2014;  
587 Gratton et al. 2018; Krienen, Yeo, and Buckner 2014). However, the vastly different temporal  
588 characteristics of fMRI and electrophysiological measures emphasize divergent types of neural processes  
589 (Hari and Parkkonen 2015; Hermes et al. 2019; Hermes, Nguyen, and Winawer 2017). fMRI-based FC  
590 represents coupling of infraslow and aperiodic fluctuations of activation amplitude. In contrast, coupling  
591 of oscillatory neural signals, especially phase coupling, represent FC mechanisms based on rapid  
592 rhythmicity.

593 The strong spatial stability in our study ( $r=0.69$ ; mean over all cross-state comparisons of phase coupling  
594 within frequencies) is especially surprising in light of the role of neural oscillations in rapid cognitive  
595 processes. This state-invariance of FC organization is missed in common electrophysiological task-based  
596 studies, as such studies typically normalize active trial processing to a pre-trial baseline or contrast task  
597 conditions in individual connections without considering the distributed spatial pattern of FC.

598 However, the observed stability leaves room for subtle or spatially confined task-specific FC changes. It  
599 is important to consider the interplay between space and time in FC dynamics. Our observation of spatial  
600 stability of FC in various cognitive contexts over the full trial duration does not preclude divergent  
601 temporal dynamics in different tasks (see discussion of time-varying dynamics below). Further, spatial

602 correspondence of FC across states was high but not perfect, suggesting the presence of task-specific  
603 adjustments. This latter observation is in line with small but task-specific changes in fMRI-based FC  
604 during particular tasks (e.g. Cohen and D'Esposito 2016). Thus, the observed spatial stability is  
605 compatible with additional minor but functionally important and task-specific changes in FC patterns.

## 606 Stability of oscillation-based FC across frequency bands

607 The cognitive state invariance of oscillation-based FC organization was observed in all canonical  
608 frequency bands from theta to high gamma, suggesting that this spatial organization is conserved across  
609 frequencies. Direct pairwise comparisons of frequency-specific intrinsic FC across frequency bands  
610 revealed highly similar FC organization across all bands ( $r = 0.69$  to  $0.88$ ). This finding is surprising,  
611 given that frequency-specific oscillation-based FC has been linked to different cognitive operations, each  
612 associated with different sets of brain areas (S. Palva and Palva 2018). For instance, theta, alpha, and  
613 gamma band oscillations (both in terms of local power and cross-region coupling) are thought to reflect  
614 navigation and memory encoding/retrieval (Backus et al. 2016), attentional processes (Sadaghiani and  
615 Kleinschmidt 2016), and local representation of item content (Rohenkohl, Bosman, and Fries 2018),  
616 respectively. These observations would suggest a frequency-specific rather than a frequency-stable  
617 spatial organization of FC (Sadaghiani and Wirsich 2019).

618 However, computer modeling studies have shown that spatial organization of static FC in various  
619 frequency bands can be largely predicted by the structural connectivity (Cabral et al. 2014; Hansen et al.  
620 2015; Schirner et al. 2018), suggesting some degree of frequency-invariance in the organization of FC.  
621 For example, Cabral and colleagues (2014) reported strong correlation between empirical FC of MEG  
622 data and time series generated from theoretical computer models informed by structural connectivity.  
623 Importantly, this observation concurrently held true for multiple oscillation frequency bands suggesting  
624 that oscillation-based FC entails a frequency-independent component. Our observation of relatively  
625 strong frequency invariance agrees with this viewpoint, whilst also permitting considerably smaller  
626 frequency-specific connectivity patterns.

## 627 Temporally independent frequency-specific FC dynamics

628 Our analysis of FC time-varying dynamics in each frequency band suggests that frequency-invariance  
629 likely reflects multiple frequency-specific coupling processes that enact a shared spatial organization,  
630 rather than a single broadband process. This finding may explain how frequency-specific task-evoked FC  
631 changes can co-exist with a frequency-invariant spatial organization. Although temporally independent  
632 FC dynamics in different frequency bands are consistent with temporally distinct task-evoked changes in  
633 each band, these results are dependent on the time frame considered. For instance, when assessing these  
634 connection-wise dynamics over more extensive observations (i.e., longer time period), the relatively  
635 unitary state- and frequency-invariant spatial organization of FC emerges at the large-scale connectivity  
636 level. Our finding is consistent with long-term EEG and ECoG recordings that report the emergence of  
637 spatial stability only at periods >100sec (Chu et al. 2012; Kramer et al. 2011). This observation  
638 reconciles the complimentary presence of cognitive state-invariance and frequency-invariance of FC  
639 spatial organization on the one hand and its state-responsive and frequency-specific short-term dynamics  
640 on the other.

## 641 Phase- vs. amplitude coupling

642 Beyond phase coupling, this study explored the correspondence of spatial FC across cognitive states and  
643 frequency bands in the other major mode of oscillation-based connectivity: amplitude coupling. While  
644 relative stability of FC organization was observed for both coupling modes, the cross-state FC  
645 dissimilarity for amplitude coupling was consistently larger than for phase coupling in all bands (Fig.  
646 6C) slightly exceeding dissimilarity within rest (Fig. 6D). This finding may suggest that amplitude  
647 coupling is modulated across cognitive contexts either to a larger degree or across more connections than  
648 phase coupling.

649 Further, we observed that task-responsiveness of phase- and amplitude coupling had a different profile  
650 over frequency bands (Fig. 6C & D). The observed profiles suggest that task-related changes in phase

651 coupling occur more readily in slower frequencies, while task-related amplitude-coupling enacts the  
652 higher frequencies more strongly. The dissociable task-related spatial reorganization emphasizes the  
653 distinctness of task-related phase- and amplitude coupling (Mostame and Sadaghiani 2020).

#### 654 Source leakage contributions

655 Could the observed state- and frequency-invariance be caused by volume conduction present in the data  
656 regardless of the cognitive state or frequency band? Although ECoG is considerably less affected by  
657 volume conduction than scalp EEG, we addressed this concern after removing zero-lag FC and distance  
658 dependence of FC. We detected a moderate reduction of the effect size of the spatial correspondence  
659 especially when suppressing zero-lag FC. Unfortunately, the conservative approach of suppressing zero-  
660 lag FC comes at the cost of removing real zero-lag connectivity whose existence (e.g., Gray et al. 1989;  
661 Rodriguez et al. 1999; Roelfsema et al. 1997) and contribution to the whole-brain connectome (e.g.,  
662 Finger et al. 2016) are supported empirically and theoretically (Viriyopase et al. 2012). Importantly  
663 however, a large proportion of the data still reflected the state-invariant FC organization, indicating that  
664 volume conduction is not a primary driver of our effects. These observations emphasize the advantage of  
665 ECoG over noninvasive neurophysiological signals for investigating FC organization under minimal  
666 volume conduction effects.

#### 667 Limitations

668 While ECoG provides a unique window into direct intracranial recordings of the human brain, it suffers  
669 from limited electrode coverage. Thus, the observed FC organization could not be directly related to  
670 previously reported whole-brain FC networks. Importantly however, the core question regarding spatial  
671 stability of FC across cognitive states and frequency bands was not contingent upon knowing the  
672 correspondence to MRI-based networks. Moreover, the variability of electrode coverage across subjects -  
673 while it prevents comparisons across subjects- suggests that our observations are robust over different  
674 sets of brain areas.

675 Another limitation of ECoG is that due to its invasive nature it is only available in patients with a history  
676 of epilepsy. In particular, electrodes coverage usually includes affected brain areas to serve clinical  
677 purposes. However, data did not include electrodes and time periods with excessive inter-ictal activity.  
678 Thus, we believe that the high SNR of ECoG and its relative insensitivity to volume conduction far  
679 outweighs this potential limitation for the purposes of studying oscillation-based FC. Thereby our study  
680 adds to the wealth of prior ECoG studies successfully informing about normal brain processes (Parvizi  
681 and Kastner 2018) and FC in particular (e.g. (Betzel et al. 2019; Kucyi et al. 2018)).

682 Another limitation ensuing from the rare opportunity of intracranial human recordings is the limited  
683 sample size. Cross-state investigations require patients with data from at least two task conditions. The  
684 overlap of *Motor* and *Rest* provided a sample size of 17 patients, which is relatively large in the context  
685 of ECoG literature. However, other tasks that we included in support of a broad representation of  
686 cognitive states were available in a subset of patients only. Nevertheless, the extraordinary SNR of  
687 intracranial recordings permits assessment of effects in individual subjects. Accordingly, the core  
688 conclusions of state- and frequency invariance were established using both group-level statistics as well  
689 as single-subject tests using subject-specific null models. The observation of all core findings in the vast  
690 majority of individual comparisons (with rigorous multiple comparisons corrections) provides strong  
691 quantitative support for the robustness of our results.

## 692 Conclusions

693 Our findings suggest that spatial organization of oscillation-based FC is shared across frequency bands  
694 and is stable across a variety of tasks and rest. Invariance of oscillation-based FC across cognitive states  
695 agrees with parallel observations of such invariance in the correlation structure of the aperiodic fMRI  
696 BOLD signal. This convergence suggests a universal phenomenon from the millisecond timescale of  
697 electrophysiology to the infraslow range of fMRI. These observations speak to conceptual frameworks of  
698 oscillation-based FC incorporating a largely state- and frequency-invariant spatial organization beyond  
699 state-responsive and frequency-specific short-term dynamics of FC (Sadaghiani and Wirsich 2019).

700 Such conceptual considerations also have important practical implications for calculating and  
701 interpreting task-based electrophysiological connectivity. This is especially important, because  
702 commonly used non-parametric statistical tests (phase permutation, Bootstrap resampling, etc.) differ in  
703 the adequacy with which their assumed null distribution captures task-independent connectivity already  
704 present in the pre-stimulus baseline (Moharramipour et al. 2018; Mostame et al. 2019). Intrinsic  
705 connectivity can be taken into account by either demeaning connectivity at each connection with respect  
706 to its corresponding baseline connectivity before statistical testing, or by employing random sampling  
707 approaches that include baseline data (Mostame et al. 2019).

708 The strong similarity of spatial FC organization across mental states also motivates dedicated studies to  
709 characterize the subtle but functionally meaningful state-dependent modulation of this distributed  
710 organization. Given sufficient spatial localizability (in either distributed intracranial data or whole-brain  
711 source-localized scalp data), comparisons between task conditions can be performed using network-  
712 based statistical approaches rather than studying individual connections (e.g. Zalesky, Fornito, and  
713 Bullmore 2010). In summary, concurrently considering the distributed spatial organization and temporal  
714 dynamics of FC in future task-based studies will be important to advance the neurobiological  
715 understanding of functional networks.

## 716 **References**

- 717 Backus, Alexander R. et al. 2016. “Hippocampal-Prefrontal Theta Oscillations Support Memory Integration.”  
718 *Current Biology* 26(4): 450–57.
- 719 Beckmann, Christian F., Marilena DeLuca, Joseph T. Devlin, and Stephen M. Smith. 2005. “Investigations  
720 into Resting-State Connectivity Using Independent Component Analysis.” *Philosophical Transactions*  
721 *of the Royal Society B: Biological Sciences* 360(1457): 1001–1013.
- 722 Berger, H. 1930. “Ueber Das Elektrenkephalogramm Des Menschen. [Electrocephalography in Man.]”  
723 *Journal für Psychologie und Neurologie* 40: 160–79.

- 724 Betzel, Richard F. et al. 2019. “Structural, Geometric and Genetic Factors Predict Interregional Brain  
725 Connectivity Patterns Probed by Electroencephalography.” *Nature Biomedical Engineering*: 1.
- 726 Brookes, Matthew J. et al. 2011. “Investigating the Electrophysiological Basis of Resting State Networks  
727 Using Magnetoencephalography.” *Proceedings of the National Academy of Sciences* 108(40): 16783–  
728 16788.
- 729 Cabral, Joana et al. 2014. “Exploring Mechanisms of Spontaneous Functional Connectivity in MEG: How  
730 Delayed Network Interactions Lead to Structured Amplitude Envelopes of Band-Pass Filtered  
731 Oscillations.” *NeuroImage* 90: 423–35.
- 732 Chu, Catherine J. et al. 2012. “Emergence of Stable Functional Networks in Long-Term Human  
733 Electroencephalography.” *Journal of Neuroscience* 32(8): 2703–13.
- 734 Cohen, Jessica R., and Mark D’Esposito. 2016. “The Segregation and Integration of Distinct Brain Networks  
735 and Their Relationship to Cognition.” *Journal of Neuroscience* 36(48): 12083–12094.
- 736 Cohen, Michael X. 2015. “Effects of Time Lag and Frequency Matching on Phase-Based Connectivity.”  
737 *Journal of Neuroscience Methods* 250: 137–46.
- 738 Colclough, G. L. et al. 2016. “How Reliable Are MEG Resting-State Connectivity Metrics?” *NeuroImage* 138:  
739 284–93.
- 740 Cole, Michael W. et al. 2014. “Intrinsic and Task-Evoked Network Architectures of the Human Brain.”  
741 *Neuron* 83(1): 238–251.
- 742 Deligianni, Fani, Maria Centeno, David W. Carmichael, and Jonathan D. Clayden. 2014. “Relating Resting-  
743 State fMRI and EEG Whole-Brain Connectomes across Frequency Bands.” *Frontiers in neuroscience*  
744 8: 258.

- 745 Dubey, Agrita, and Supratim Ray. 2019. “Cortical Electrocochogram (ECoG) Is a Local Signal.” *Journal of*  
746 *Neuroscience* 39(22): 4299–4311.
- 747 Engel, Andreas K., Christian Gerloff, Claus C. Hilgetag, and Guido Nolte. 2013. “Intrinsic Coupling Modes:  
748 Multiscale Interactions in Ongoing Brain Activity.” *Neuron* 80(4): 867–86.
- 749 Fell, Juergen, and Nikolai Axmacher. 2011. “The Role of Phase Synchronization in Memory Processes.”  
750 *Nature Reviews Neuroscience* 12(2): 105–18.
- 751 Finger, Holger et al. 2016. “Modeling of Large-Scale Functional Brain Networks Based on Structural  
752 Connectivity from DTI: Comparison with EEG Derived Phase Coupling Networks and Evaluation of  
753 Alternative Methods along the Modeling Path.” *PLoS computational biology* 12(8): e1005025.
- 754 Fox, Kieran CR et al. 2018. “Intracranial Electrophysiology of the Human Default Network.” *Trends in*  
755 *cognitive sciences*.
- 756 Fox, Michael D., and Marcus E. Raichle. 2007. “Spontaneous Fluctuations in Brain Activity Observed with  
757 Functional Magnetic Resonance Imaging.” *Nature Reviews Neuroscience* 8(9): 700–711.
- 758 Gratton, Caterina et al. 2018. “Functional Brain Networks Are Dominated by Stable Group and Individual  
759 Factors, Not Cognitive or Daily Variation.” *Neuron* 98(2): 439-452.e5.
- 760 Gray, Charles M., Peter König, Andreas K. Engel, and Wolf Singer. 1989. “Oscillatory Responses in Cat  
761 Visual Cortex Exhibit Inter-Columnar Synchronization Which Reflects Global Stimulus Properties.”  
762 *Nature* 338(6213): 334–37.
- 763 Gruber, Matthias J. et al. 2018. “Theta Phase Synchronization between the Human Hippocampus and  
764 Prefrontal Cortex Increases during Encoding of Unexpected Information: A Case Study.” *Journal of*  
765 *Cognitive Neuroscience* 30(11): 1646–56.

- 766 Hansen, Enrique C. A. et al. 2015. “Functional Connectivity Dynamics: Modeling the Switching Behavior of  
767 the Resting State.” *NeuroImage* 105: 525–35.
- 768 Hari, Riitta, and Lauri Parkkonen. 2015. “The Brain Timewise: How Timing Shapes and Supports Brain  
769 Function.” *Philosophical Transactions of the Royal Society B: Biological Sciences* 370(1668):  
770 20140170.
- 771 Hearne, Luke J., Luca Cocchi, Andrew Zalesky, and Jason B. Mattingley. 2017. “Reconfiguration of Brain  
772 Network Architectures between Resting-State and Complexity-Dependent Cognitive Reasoning.”  
773 *Journal of Neuroscience* 37(35): 8399–8411.
- 774 Hermes, Dora, Mai Nguyen, and Jonathan Winawer. 2017. “Neuronal Synchrony and the Relation between the  
775 Blood-Oxygen-Level Dependent Response and the Local Field Potential.” *PLOS Biology* 15(7):  
776 e2001461.
- 777 Hermes, Dora, Natalia Petridou, Kendrick N Kay, and Jonathan Winawer. 2019. “An Image-Computable  
778 Model for the Stimulus Selectivity of Gamma Oscillations” ed. Saskia Haegens. *eLife* 8: e47035.
- 779 van den Heuvel, Martijn P., and Hilleke E. Hulshoff Pol. 2010. “Exploring the Brain Network: A Review on  
780 Resting-State fMRI Functional Connectivity.” *European Neuropsychopharmacology* 20(8): 519–34.
- 781 Hillebrand, Arjan et al. 2012. “Frequency-Dependent Functional Connectivity within Resting-State Networks:  
782 An Atlas-Based MEG Beamformer Solution.” *Neuroimage* 59(4): 3909–3921.
- 783 Hipp, Joerg F., and Markus Siegel. 2015. “BOLD fMRI Correlation Reflects Frequency-Specific Neuronal  
784 Correlation.” *Current Biology* 25(10): 1368–1374.
- 785 Jensen, Ole, Bart Gips, Til Ole Bergmann, and Mathilde Bonnefond. 2014. “Temporal Coding Organized by  
786 Coupled Alpha and Gamma Oscillations Prioritize Visual Processing.” *Trends in Neurosciences* 37(7):  
787 357–69.

- 788 Kanda, Paulo Afonso de Medeiros et al. 2009. “The Clinical Use of Quantitative EEG in Cognitive Disorders.”  
789 *Dementia & Neuropsychologia* 3(3): 195–203.
- 790 Khanna, Preeya, and Jose M Carmena. 2015. “Neural Oscillations: Beta Band Activity across Motor  
791 Networks.” *Current Opinion in Neurobiology* 32: 60–67.
- 792 Kramer, Mark A. et al. 2011. “Emergence of Persistent Networks in Long-Term Intracranial EEG  
793 Recordings.” *Journal of Neuroscience* 31(44): 15757–67.
- 794 Krienen, Fenna M., BT Thomas Yeo, and Randy L. Buckner. 2014. “Reconfigurable Task-Dependent  
795 Functional Coupling Modes Cluster around a Core Functional Architecture.” *Philosophical  
796 Transactions of the Royal Society B: Biological Sciences* 369(1653): 20130526.
- 797 Kucyi, Aaron et al. 2018. “Intracranial Electrophysiology Reveals Reproducible Intrinsic Functional  
798 Connectivity within Human Brain Networks.” *The Journal of Neuroscience* 38(17): 4230–42.
- 799 Lachaux, Jean-Philippe, Eugenio Rodriguez, Jacques Martinerie, and Francisco J. Varela. 1999. “Measuring  
800 Phase Synchrony in Brain Signals.” *Human brain mapping* 8(4): 194–208.
- 801 Miller, Kai J. et al. 2007. “Spectral Changes in Cortical Surface Potentials during Motor Movement.” *Journal  
802 of Neuroscience* 27(9): 2424–32.
- 803 ———. 2012. “Human Motor Cortical Activity Is Selectively Phase-Entrained on Underlying Rhythms.”  
804 *PLOS Computational Biology* 8(9): e1002655.
- 805 ———. 2019. “A Library of Human Electrographic Data and Analyses.” *Nature Human Behaviour*  
806 3(11): 1225–35.
- 807 Miller, Kai J., Larry B. Sorensen, Jeffrey G. Ojemann, and Marcel den Nijs. 2009. “Power-Law Scaling in the  
808 Brain Surface Electric Potential.” *PLOS Computational Biology* 5(12): e1000609.

- 809 Mostame, Parham, Ali Moharramipour, Gholam-Ali Hossein-Zadeh, and Abbas Babajani-Feremi. 2019.  
810 “Statistical Significance Assessment of Phase Synchrony in the Presence of Background Couplings: An  
811 ECoG Study.” *Brain Topography*. <https://doi.org/10.1007/s10548-019-00718-8> (July 8, 2019).
- 812 Mostame, Parham, and Sepideh Sadaghiani. 2020. “Phase- and Amplitude-Coupling Are Tied by an Intrinsic  
813 Spatial Organization but Show Divergent Stimulus-Related Changes.” *NeuroImage* 219: 117051.
- 814 Nentwich, Maximilian et al. 2020. “Functional Connectivity of EEG Is Subject-Specific, Associated with  
815 Phenotype, and Different from FMRI.” *NeuroImage* 218: 117001.
- 816 Nolte, Guido et al. 2004. “Identifying True Brain Interaction from EEG Data Using the Imaginary Part of  
817 Coherency.” *Clinical neurophysiology* 115(10): 2292–2307.
- 818 Oostenveld, Robert, Pascal Fries, Eric Maris, and Jan-Mathijs Schoffelen. 2011. “FieldTrip: Open Source  
819 Software for Advanced Analysis of MEG, EEG, and Invasive Electrophysiological Data.” *Intell.*  
820 *Neuroscience* 2011: 1:1–1:9.
- 821 Palva, J. Matias et al. 2018. “Ghost Interactions in MEG/EEG Source Space: A Note of Caution on Inter-Areal  
822 Coupling Measures.” *NeuroImage* 173: 632–43.
- 823 Palva, Satu, and J. Matias Palva. 2007. “New Vistas for  $\alpha$ -Frequency Band Oscillations.” *Trends in*  
824 *Neurosciences* 30(4): 150–58.
- 825 ———. 2018. “Roles of Brain Criticality and Multiscale Oscillations in Temporal Predictions for  
826 Sensorimotor Processing.” *Trends in Neurosciences* 41(10): 729–43.
- 827 Parvizi, Josef, and Sabine Kastner. 2018. “Promises and Limitations of Human Intracranial  
828 Electroencephalography.” *Nature Neuroscience* 21(4): 474–83.
- 829 Petersen, Steven E., and Olaf Sporns. 2015. “Brain Networks and Cognitive Architectures.” *Neuron* 88(1):  
830 207–19.

- 831 Prichard, Dean, and James Theiler. 1994. “Generating Surrogate Data for Time Series with Several  
832 Simultaneously Measured Variables.” *Physical Review Letters* 73(7): 951–54.
- 833 Rimmele, Johanna M., Joachim Gross, Sophie Molholm, and Anne Keitel. 2018. “Editorial: Brain Oscillations  
834 in Human Communication.” *Frontiers in Human Neuroscience* 12.  
835 <https://www.frontiersin.org/articles/10.3389/fnhum.2018.00039/full> (January 31, 2020).
- 836 Rodriguez, Eugenio et al. 1999. “Perception’s Shadow: Long-Distance Synchronization of Human Brain  
837 Activity.” *Nature* 397(6718): 430–33.
- 838 Roelfsema, Pieter R., Andreas K. Engel, Peter König, and Wolf Singer. 1997. “Visuomotor Integration Is  
839 Associated with Zero Time-Lag Synchronization among Cortical Areas.” *Nature* 385(6612): 157–61.
- 840 Rogers, Nicholas et al. 2019. “Correlation Structure in Micro-ECoG Recordings Is Described by Spatially  
841 Coherent Components.” *PLOS Computational Biology* 15(2): e1006769.
- 842 Rohenkohl, Gustavo, Conrado Arturo Bosman, and Pascal Fries. 2018. “Gamma Synchronization between V1  
843 and V4 Improves Behavioral Performance.” *Neuron* 100(4): 953-963.e3.
- 844 Rouse, A. G., J. J. Williams, J. J. Wheeler, and D. W. Moran. 2016. “Spatial Co-Adaptation of Cortical  
845 Control Columns in a Micro-ECoG Brain–Computer Interface.” *Journal of Neural Engineering* 13(5):  
846 056018.
- 847 Sadaghiani, Sepideh et al. 2012. “Alpha-Band Phase Synchrony Is Related to Activity in the Fronto-Parietal  
848 Adaptive Control Network.” *The Journal of neuroscience: the official journal of the Society for*  
849 *Neuroscience* 32(41): 14305–10.
- 850 ———. 2019. “Lesions to the Fronto-Parietal Network Impact Alpha-Band Phase Synchrony and Cognitive  
851 Control.” *Cerebral Cortex* 29(10): 4143–53.

- 852 Sadaghiani, Sepideh, and Andreas Kleinschmidt. 2013. “Functional Interactions between Intrinsic Brain  
853 Activity and Behavior.” *NeuroImage* 80: 379–86.
- 854 ———. 2016. “Brain Networks and  $\alpha$ -Oscillations: Structural and Functional Foundations of Cognitive  
855 Control.” *Trends in Cognitive Sciences* 20(11): 805–17.
- 856 Sadaghiani, Sepideh, and Jonathan Wirsich. 2019. “Intrinsic Connectome Organization across Temporal  
857 Scales: New Insights from Cross-Modal Approaches.” *Network Neuroscience*: 1–49.
- 858 Schirner, Michael et al. 2018. “Inferring Multi-Scale Neural Mechanisms with Brain Network Modelling” ed.  
859 Charles E Schroeder. *eLife* 7: e28927.
- 860 Schoffelen, Jan-Mathijs, and Joachim Gross. 2009. “Source Connectivity Analysis with MEG and EEG.”  
861 *Human Brain Mapping* 30(6): 1857–65.
- 862 Singer, Wolf. 1999. “Neuronal Synchrony: A Versatile Code for the Definition of Relations?” *Neuron* 24(1):  
863 49–65.
- 864 ———. 2013. “Cortical Dynamics Revisited.” *Trends in Cognitive Sciences* 17(12): 616–26.
- 865 Smith, Stephen M. et al. 2009. “Correspondence of the Brain’s Functional Architecture during Activation and  
866 Rest.” *Proceedings of the National Academy of Sciences* 106(31): 13040–45.
- 867 Sockeel, Stéphane, Denis Schwartz, Mélanie Pélégriani-Issac, and Habib Benali. 2016. “Large-Scale Functional  
868 Networks Identified from Resting-State EEG Using Spatial ICA.” *PloS one* 11(1): e0146845.
- 869 Tewarie, P. et al. 2016. “Predicting Haemodynamic Networks Using Electrophysiology: The Role of Non-  
870 Linear and Cross-Frequency Interactions.” *Neuroimage* 130: 273–92.
- 871 Thompson, William Hedley, and Peter Fransson. 2015. “The Frequency Dimension of fMRI Dynamic  
872 Connectivity: Network Connectivity, Functional Hubs and Integration in the Resting Brain.”  
873 *NeuroImage* 121: 227–42.

- 874 Uhlhaas, Peter et al. 2009. “Neural Synchrony in Cortical Networks: History, Concept and Current Status.”  
875 *Frontiers in integrative neuroscience* 3: 17.
- 876 VanRullen, Rufin. 2016. “Perceptual Cycles.” *Trends in Cognitive Sciences* 20(10): 723–35.
- 877 Varela, Francisco, Jean-Philippe Lachaux, Eugenio Rodriguez, and Jacques Martinerie. 2001. “The Brainweb:  
878 Phase Synchronization and Large-Scale Integration.” *Nature reviews neuroscience* 2(4): 229.
- 879 Viriyopase, Atthaphon, Ingo Bojak, Magteld Zeitler, and Stan Gielen. 2012. “When Long-Range Zero-Lag  
880 Synchronization Is Feasible in Cortical Networks.” *Frontiers in Computational Neuroscience* 6.  
881 <https://www.frontiersin.org/articles/10.3389/fncom.2012.00049/full> (January 2, 2020).
- 882 Wirsich, Jonathan et al. 2017. “Complementary Contributions of Concurrent EEG and FMRI Connectivity for  
883 Predicting Structural Connectivity.” *NeuroImage* 161: 251–260.
- 884



